Lasers in Surgery and Medicine 20:310–318 (1997)

Quantitative Measurements of Linear Birefringence During Heating of Native Collagen

Duncan J. Maitland, PhD,[2]* and Joseph T. Walsh, Jr., PhD[1]

[1]Biomedical Engineering Department, Northwestern University, Evanston, Illinois 60208
[2]Lawrence Livermore National Laboratory, Livermore, California 94550

Background and Objective: **Linear birefringence is an anisotropic property of rat tail tendon, which is largely composed of collagen. Our goal is to show that the dynamic range and sensitivity of the linear birefringence loss of collagen during heating are sufficient for kinetic modeling of the reaction.**
Study Design, Materials and Methods: **The linear birefringence loss was quantified for tendon denatured via both a heated-isotonic-saline bath and a heated stage. All measurements were made with a polarizing transmission microscope equipped with a Berek compensator.**
Results: **The data show that the loss of linear birefringence is a first-order kinetic reaction. The native rat tail tendon birefringence, $\Delta n = 3.0 \pm 0.6 \times 10^{-3}$ (mean ± std. err.), is lost after denaturation occurs ($\Delta n = 0$). Application of the Arrhenius equation to the linear birefringence data yields the activation energy ($E_a = 89 \pm 1$ kcal/mole), pre-exponential coefficient ($A = e^{130\pm1}$ s^{-1}), enthalpy ($\Delta H = 88 \pm 1$ kcal/mole) and entropy ($\Delta S = 197 \pm 2$ cal/°K·mole).**
Conclusion: **This study shows that dynamic changes in linear birefringence can be used to monitor thermally induced changes in collagen. Lasers Surg. Medicine 20:310–318, 1997.**

Key words: anisotropic optical properties of tissue; polarized light; dynamic changes in optical properties; rat tail tendon; entropy; enthalpy; Arrhenius; first-order kinetic reaction

INTRODUCTION

Thermally induced changes in tissue birefringence hold promise as a feedback parameter for clinical procedures that require real-time monitoring of the thermal/mechanical state of tissue, such as corneal keratoplasty and tissue welding. In this report, we demonstrate that changes in birefringence indicate the onset and temporal progress of thermal denaturation during heating of tissue. Also, our data indicate that multiple kinetic reactions are present during collagen denaturation.

Historically, birefringence has been a tool for the histologic identification of thermal-damage zones in tissue [1]. More recently, birefringence has been used to quantify the relative conformational state of heated tissues. For example, the loss of linear birefringence has been used to determine the kinetic parameters required to model the thermal denaturation of canine myocardium [2,3] and rat skin [4]. Each of these reports concludes that the denaturation of collagen results in a loss of tissue birefringence following

Contract grant sponsor: NSF Young Investigator Award; Contract grant number: BCS-9257492; Contract grant sponsor: NSF; Contract grant number: BCS-9222483; Contract grant sponsor: NIH; Contract grant number: R01GM50534; Contract grant sponsor: MRSEC Program of the NSF; Contract grant number: DMR-9120521.

*Correspondence to: Duncan J. Maitland, Medical Photonics Laboratory, Lawrence Livermore National Laboratory, P.O. Box 808, L-399, Livermore, CA 94551.

Accepted for publication 29 December 1995.

sufficient heating. We used standard crystallography techniques to quantify dynamic changes in tissue birefringence during heating of rat tail tendons [5,6]. We compare our results with those obtained using optical and nonoptical measures of thermally induced changes in collagen based tissues, and we speculate that real-time measurements of birefringence changes can be used to monitor or control tissue heating protocols.

Linear Birefringence

Linear birefringence is a polarization specific electromagnetic property of materials. When linearly polarized light propagates in a linearly anisotropic medium, the speed of light in the medium is a function of the electric field orientation of the traveling wave relative to the optical axes of the medium. The refractive indices of an anisotropic medium can be represented by n_1, n_2, and n_3. For a uniaxial crystal, $n_1 \neq n_2 = n_3$; for a biaxial crystal, $n_1 \neq n_2 \neq n_3$. If the medium's optical axes are orthogonal, it is common to replace the ambiguous subscripts with standard Cartesian coordinate subscripts (e.g. n_x, n_y, n_z). The optical axes of collagen are orthogonal, thus Cartesian subscripts are used.

If linearly polarized light is introduced into an anisotropic medium, the orthogonal components of the electric field will experience different refractive indices, assuming that the plane of polarization of the incident light is not parallel to one of the medium's optical axes. Since the orthogonal electric field components travel at different velocities, the field components experience a phase shift relative to one another. The phase shift, δ, can be represented by [5,7],

$$\delta = \frac{2\pi d \Delta n}{\lambda_o} \tag{1}$$

where, δ is the phase shift between propagating orthogonal linear polarizations (radians), d is the sample thickness (μm), Δn is the refractive index difference between two of the optical axes in an anisotropic sample (dimensionless), and λ_o is the wavelength of light in a vacuum (μm). The traditional method for quantifying the phase shift caused by a birefringent medium is manual nulling of the medium's induced phase shift, δ_{medium}, with a second, calibrated, anisotropic crystal of variable phase shift set such that $\delta_{null} = -\delta_{medium}$. This phase compensation technique is well described in crystallography texts [5,6]. A derivation of the phase shift and resulting transmission intensity for various polarizer-sample-analyzer configurations is given by Jerrard [7]. A practical guide for polarized light microscopy is well presented in the brochure written by Patzelt [8].

Collagen

Collagen's rodlike triple helix conformation results in both linear and circular anisotropic properties [9,10]. Thus, collagen is a linearly birefringent tissue constituent. The fundamental building block of collagen fibers is the tropocollagen molecule. Tropocollagen is comprised of three lefthanded α-helices that combine to form a single righthanded super helix. The collagen fiber is formed from a staggered array of the tropocollagen molecules. The molecular packing structure of a collagen fiber is such that the refractive index along a fiber's length is greater than the crossectional refractive index [10–12]. Thus native collagen type I has a uniaxial semicrystalline conformation, where the refractive index parallel to the length of a tendon is larger than the refractive index along any orthogonal axes in the plane of the tendon's crossection. Hence, for native rat tail tendon (RTT), $n_z > n_x = n_y$.

Yoshioka and O'Konski [10] reported $n_z - n_x = \Delta n = 1.2 \times 10^{-6}$ for tropocollagen, extracted from RTT, in a 0.022 g/l dilute solution of collagen in 0.0029 molar acetic acid. Naylor found a lamellae birefringence of $\Delta n = 3.0 \times 10^{-3}$ from in vitro cat cornea [11]. Further, he showed, via immersion techniques, that ~30% of the lamellae linear birefringence is intrinsic. Thus stromal birefringence is 70% form and 30% structural (intrinsic), where structural birefringence is due to molecular anisotropy and form birefringence is a result of anisotropic alignment of molecules (individually isotropic or anisotropic) in an isotropic ground substance.

Van Blokland and Verhelst [12] have reported the birefringence of human cornea in vivo to be $\Delta n = 1.59 \times 10^{-3}$. This birefringence value agrees well with the observations of Stanworth and Naylor [13], who showed that bovine lamellae birefringence is 2.8×10^{-3} and whole cornea birefringence is one-half of the lamellae birefringence due to the random orientation of the lamellae.

Thermal Denaturation of Collagen

Upon heating, the transition by collagen from an α-helix, which can be viewed as rodlike, to a random-coil conformation is accompanied by

a loss of birefringence. Several previous investigations have provided insight to why the loss of birefringence occurs. E.R. Blout et al. [14] showed that an order of magnitude loss in optical rotary dispersion occurs near 190 nm in solubilized collagen denatured at 50°C for 30 min. (Optical rotary dispersion is the wavelength-dependent effect of optical activity (OA). Similar to linear birefringence, OA—sometimes referred to as circular birefringence—is the difference in refractive index as measured by right-circularly polarized vs. left-circularly polarized light; i.e., $OA = 2\pi d(|n_R - n_L|)/\lambda_o$.) Other investigators have shown a similar loss of optical rotary dispersion for tropocollagen and procollagen in solution [15, 16]. Thus it is evident that tropocollagen loses some of its helical rodlike structure when thermally denatured. Further, since the macromolecule's intrinsic birefringence is a function of its rodlike conformation, a decrease in Δn is consistent with changes in the α-helix due to denaturation.

MATERIALS AND METHODS

Linear birefringence measurements of rat tail tendon (RTT) were made using a polarizing transmission microscope (Leitz Ortholux Polarizing Microscope). RTT was chosen for its high collagen type I composition and the axial alignment of collagen within the tail tendon. The phase shift, δ, was measured with a Berek compensator (dynamic range: $0 \leq \delta_{null} \leq 8\pi$). Phase shift measurement errors were ~10%. The sample thickness was measured by using the calibrated fine focus on the microscope to focus on the sample surface and then on the glass slide immediately beneath the sample. Objective lenses of 20× and 32× magnifications were used in linear birefringence and thickness measurements. Thickness measurement errors introduced due to the objective lenses' depth of field were < 10% of the tendon thickness ($d \geq 100$ μm). The birefringence, Δn, was calculated from equation 1 using the measured δ and d values. Phase shift measurements were made using white light (100 W quartz halogen source), which was assumed, for the calculation of Δn, to have a center spectral wavelength, λ_o, of 550 nm.

Samples were acquired from freshly sacrificed 3-month-old Sprage Dawley rats. Tendons were cleaned and rinsed in isotonic saline. Linear birefringence measurements were made within 48 hr post mortum. Prior to the linear birefringence measurements, samples were stored at 5°C in isotonic saline.

Two sample-heating procedures were used. In the first procedure, average linear birefringence measurements were made from RTT samples heated for 15 min in a constant-temperature isotonic saline bath. During heating, the bath temperature was maintained within ± 0.5°C. At each temperature, three tendon samples, which were randomly selected from not less than five rats, were placed in a porous plastic tissue holder (Curtis Matheson Scientific, CMS No. 244) and immersed in the saline bath. After the heating period, the denaturation was arrested by immersing the samples in a room-temperature isotonic saline bath. Two linear-birefringence measurements were made at ten different locations for three different tendon samples. Thus at each temperature, 60 phase shift measurements were taken. Three thickness measurements were made at each location and averaged for the Δn calculations. Thus the first procedure yielded Δn values for native and denatured RTT.

For the second procedure, a hot stage, with heating plates both above and below the sample (Mettler FP82 Hot Stage with a FP80 Central Processor; ambient to 300.0 ± 0.1°C), was used to control the temperature of the sample while on the microscope stage. Linear birefringence measurements were made while the samples were heated. Desiccation of the sample during heating was prevented by maintaining a small volume of isotonic saline around the sample. A 200-μm-thick Teflon spacer surrounded the sample on the microscope slide. The sample was then covered with a standard cover glass slide. The seal formed between the Teflon spacer and the two glass slides prevented most of the water from evaporating; thus the sample remained moist during heating. For a given heating temperature, T_{heat}, two phase-shift measurements and one thickness measurement were made every minute for 15 min after T_{heat} was applied. The rise time to T_{heat} was < 30 sec for temperature steps < 20°C. Therefore, in order to minimize the rise time to T_{heat}, the hot stage temperature was stabilized for ~2 min at an intermediate temperature of 40°C before increasing the temperature to T_{heat}. Initial studies showed that the intermediate temperature had no effect on the linear birefringence of the RTT samples. This heating technique allowed for the interactive measurement of linear birefringence at a single site on the tendon during various time-temperature histories, which allowed the calcula-

tion of the activated-state thermodynamic parameters: entropy (ΔS) and enthalpy (ΔH).

The application of the Arrhenius equation to the $\Delta n(T_{heat})$-vs.-time data allows the calculation of ΔS and ΔH. The Arrhenius equation, as presented by Price and Dwek [17] and Birngruber [18], is given by,

$$k = Ae^{-\frac{E_a}{RT}}, \tag{2}$$

$$A = \frac{KT}{h} e^{\frac{\Delta S}{R}+1}, \tag{3}$$

$$E_a = \Delta H - RT, \text{ (1st order reaction)} \tag{4}$$

where; A is the pre-exponential factor s^{-1}—for a first-order reaction: or the same units as the reaction rate constant, *k,* for higher order reactions; E_a is the activation energy, cal/mole; T is the temperature, °K; R is the universal gas constant, 1.986 cal/(mole·°K); h is Plank's constant, 1.584×10^{-34} cal·s; K is Boltzman's constant, 3.298×10^{-24} cal/°K. Here, the rate constant is used instead of the more familiar damage integral as presented by Welch [19]. Calculating the rate constant as an intermediate step toward the final computation of ΔS and ΔH provides several benefits over the damage integral version of the Arrhenius equation. These issues are addressed under Discussion.

For a first-order reaction, *k* is defined as the change in the concentration of the native protein with respect to time, divided by the initial protein concentration. Following page 101 of Price and Dwek [17], this definition can be mathematically represented by,

$$k = -\frac{1}{[N_o]} \frac{d[N(t)]}{dt} s^{-1}, \tag{5}$$

where [N(t)] refers to the concentration of native collagen and $[N_o]$ is [N(t = 0)]. The integration of equation 5 leads to

$$\ln \frac{[N(t)]}{[N_o]} = -kt + c. \tag{6}$$

If the linear birefringence is assumed to be proportional to [N(t)], then

$$\ln \frac{\Delta n}{\Delta n_o} = -kt + c. \tag{7}$$

A plot of equation 7 for various Δn-vs.-time data results in a straight line of slope $-k$ if the loss of Δn is indicative of a first-order, single-rate kinetic reaction. Thus visual inspection and statistical tests of the linear-regression fit provide confirmation of the reaction order and number.

Once $k \pm$ std. err. has been calculated for a series of heating temperatures, the kinetic parameters can be found by applying the natural logarithm of equation 2, which leads to

$$\ln k = -\frac{E_a}{R}\left(\frac{1}{T}\right) + \ln A. \tag{8}$$

E_a and A can be obtained by plotting $\ln(k)$-vs.-1/T. A weighted least-squares fit of the data provides a slope ($= -E_a/R$) and y-intercept ($= \ln A$). The weighted least-squares algorithm is described by many statistical texts (cf. Draper and Smith [20]). With E_a and A known, ΔS and ΔH can be calculated from equations (3) and (4), respectively.

RESULTS

The average Δn data for RTT heated for 15 min in a water bath are presented in Figure 1. The data are presented as the difference in the refractive indices, Δn, which is independent of thickness, rather than the phase, δ, which is thickness dependent. The average data in Figure 1 provide the ranges within which the collagen's Δn values are expected to fall. Based on the transmission microscopy experiments, an order of magnitude change in Δn can be expected.

Normalized data for a series of single-site, single-temperature, time-temperature histories are presented in Figure 2. T_{heat} was applied at time equal to zero minutes. No significant loss of birefringence (i.e., significant defined as >5% loss) occurred for any of the samples during the heating period between room temperature and T_{heat}, except for T_{heat} equal to 60°C, which showed an 8% loss in Δn during the 30-sec rise time. Significant changes in Δn versus time occur for $50°C \leq T_{heat} \leq 60°C$. After heating the samples for 15 min and then air-cooling the samples to room temperature, no change in linear birefringence occurred relative to the Δn value measured at time equal to 15 min.

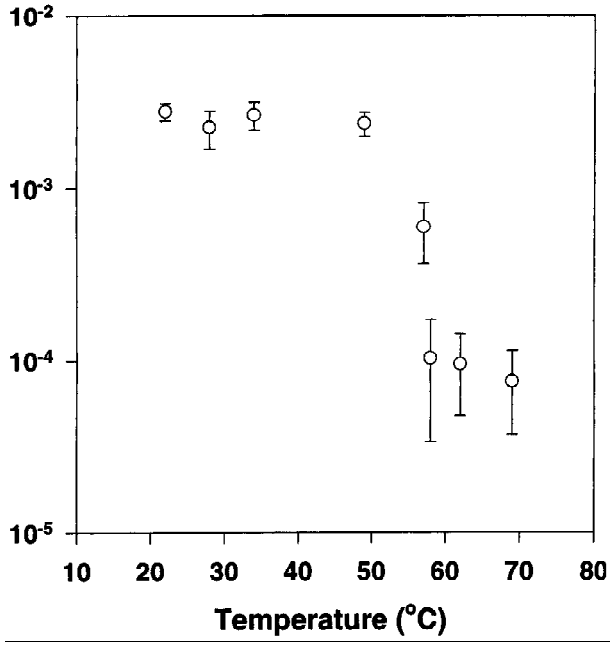

Fig. 1. Average Δn for RTT. RTT samples were heated in isotonic saline for 15 min and then immediately cooled to room temperature. Each data point is the mean ± standard deviation of 60 phase shift measurements.

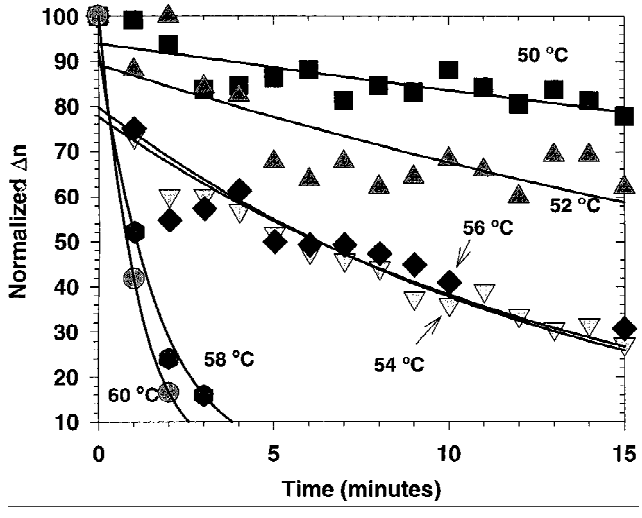

Fig. 2. Temporal changes in the linear birefringence of RTT collagen. The RTT was heated form the baseline temperature to T_{heat} in ~30 sec. Once the RTT was at T_{heat} ± 0.2°C, i.e., at time = 0, linear birefringence was measured every 60 sec. The solid lines represent a first-order exponential fit to the data, see equation 10.

Kinetic rate coefficients for the six heating temperatures shown in Figure 2 were obtained from the negative slope of the least-squares regression of the ln(Δn)-vs.-time data. The rate coefficient results are shown in Table 1 with the

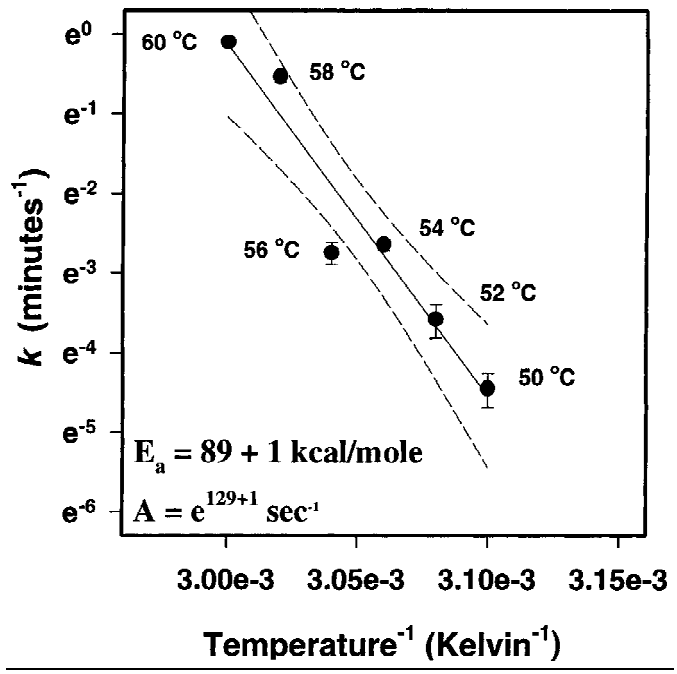

Fig. 3. Rate constant for the loss of RTT birefringence as a function of temperature. The data points (●) shown here are from Table 1 and plotted according to equation 8. The standard error of each data point is indicated by the error bars. A weighted least-squares regression yields the best-fit solid line (—); the dashed lines (---) represent the 95% confidence intervals. The kinetic parameters, E_a and A, were found from the linear regression slope and y-intercept, respectively.

statistical r values. Application of an F-test results in $P < 0.05$ for each of the six data sets.

A plot of the Arrhenius equation (see equation 8) shown in Figure 3, results in $A = e^{129.6\pm1.2}$ (s^{-1}) and $E_a = 88.5 \pm 0.8$ kcal/mole. Entropy and enthalpy are calculated from equations (3) and (4), respectively, which lead to the calculated kinetic parameters: $\Delta S = 196.7 \pm 2.4$ cal/°K·mole and $\Delta H = 87.9 \pm 0.8$ kcal/mole.

DISCUSSION

The data show that the thermal denaturation of RTT results in the loss of linear birefringence. In general, the birefringence data agree well with previous investigations. Comparisons of our data with results from other investigators is presented below where the kinetics is emphasized. The kinetic analysis, which indicates that the birefringence loss is not a simple two-state reaction, leads one to hold suspect the assumptions implicit to the damage integral formulation of the Arrhenius equation. A hypothesis for a

TABLE 1. Single-rate Kinetic Coefficients for RTT

T (°C)	k (min^{-1})	±S.E. (min^{-1})	r
50.0	0.012	0.002	−0.79
52.0	0.028	0.006	−0.79
54.0	0.071	0.005	−0.97
56.0	0.064	0.009	−0.92
58.0	0.585	0.039	−0.99
60.0	0.903	0.019	−0.99

multirate kinetic loss of birefringence is also presented.

Our measured values for the native linear birefringence of collagen type I, $\Delta n = 3.0 \times 10^{-3} \pm 0.6 \times 10^{-3}$, agree with values reported by other investigators, $\Delta n \cong 3.0 \times 10^{-3}$ [11–13]. If it is assumed that Δn equals zero for completely denatured collagen, then a linear birefringence measurement has a dynamic range of $0 \leq \Delta n \leq 3 \times 10^{-3}$. The variability in the measured Δn values is indicated in Figure 1. The cause of the increasingly larger standard deviations at higher temperatures is, in part, the accuracy of the Berek compensator. The Berek compensator is optimally used over the phase shift range $\pi \leq \delta \leq 8\pi$, with a sensitivity of 0.2% [8]. The initial (native) phase shift of RTT falls within this range. As the collagen is denatured, the phase shift decreases from its native value to zero. Over the phase shift range $0 \leq \delta \leq \pi$, the Berek compensator's error becomes increasingly larger as smaller phase shifts are measured. This inaccuracy could be corrected for by changing the compensator when the phase shift decreased below π but, at the time of experimentation, a Sénarmont compensator ($0 \leq \delta \leq \pi$) was not available to us.

After cooling the RTT to ambient temperature, no hysteresis of the linear birefringence was seen. That is, the RTT did not regain any linear birefringence with respect to the last measured Δn value prior to cooling. This implies that structural conformation pertinent to linear anisotropy is not recoverable, unlike optical activity. Cohen has shown that optical activity decreases during heating but is regained after the collagen is cooled [9]. Thus since optical activity is a function of helical conformation, some localized helical formation must occur after cooling. Additional discussions regarding the conformational basis of linear birefringence are presented below.

The Arrhenius equation-based analysis of the linear birefringence data provides thermodynamic parameters useful in kinetic modeling of the collagen-denaturation process (see equations 2–4). One can calculate thermodynamic parameters from the time-temperature birefringence data via two, distinct, Arrhenius-equation-based methods. The first standard technique involves two steps: (1) determination of the reaction rate constants at different heating temperatures and then, (2) calculation of the thermodynamic parameters from the slope and y-intercept of ln(k)-vs.-1/T. This method has the benefit of identifying nonfirst-order or multiple reaction by visual examination of a plot of Δn-vs.-time (i.e., equation 7). The second Arrhenius-based technique uses the damage integral,

$$\Omega = \int k\, dt = \frac{K}{h} e^{\left(\frac{\Delta S}{R}+1\right)} \int_{t_{start}}^{t_{final}} T(t) e^{-\left(\frac{E_a}{RT(t)}\right)} dt. \tag{9}$$

which is the integration of equation 2 with respect to time. The use of the damage integral in kinetic analysis of time-temperature data dominates the tissue-optics field. The thermodynamic parameters are reduced from the time-temperature birefringence data by obtaining the slope and y-intercept from a plot of ln(t*)-vs.-1/T, where t* is the time for, say, a 63% loss of birefringence. The damage integral assumes that the reaction is a two-state, single-rate reaction. As expected, the two methodologies result in the same thermodynamic parameters for a two-state, single-rate system. We have chosen to use the two-step, kinetic rate formulation of the Arrhenius equation in our analysis.

The application of the kinetic rate analysis to the birefringence data can be seen in Figure 2. The fit of equation 7 is shown against the time-temperature data. For the sake of this discussion, the scaling of Figure 2 uses a rearrangement of equation 7,

$$\frac{\Delta n(t)}{\Delta n_o} = Ce^{-kt}, \tag{10}$$

where the fitted parameters are the exponential time constant, k, and the proportionality constant, C. Clearly, Figure 2 indicates that the birefringence loss is not well described by a two-state (i.e., native → denatured), single-rate (i.e., k) reaction. The single-exponential fit fails to predict both the exponential decay and y-intercept (proportionality constant) of the data, especially at low heating temperatures.

A better visualization of these observations

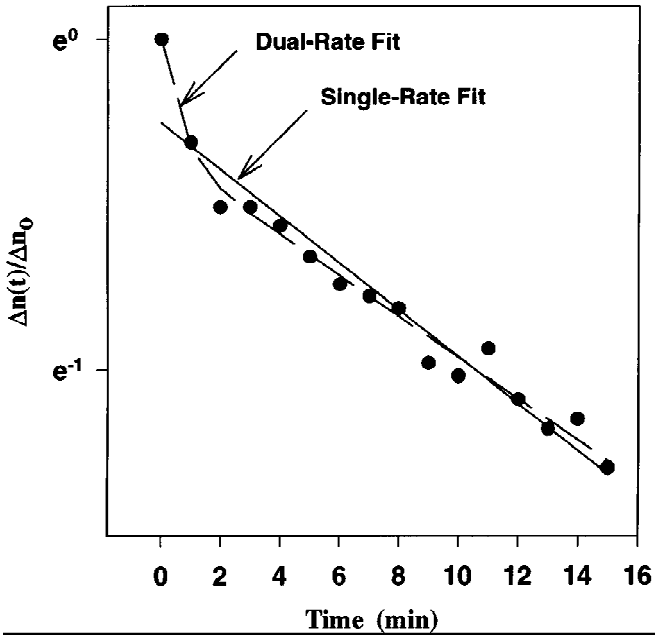

Fig. 4. Comparison of single-rate and dual-rate kinetic models. The 54°C data from Figure 2 is shown on a semilogarithmic plot of relative birefringence-vs.-time. The dual-rate fit properly fits both the y-intercept as well as the change in slope of the data.

is available in Figure 4 where a semilogarithmic plot of the 54°C data from Figure 2 is shown. The single-rate fit of the data is shown along with a dual-rate fit of the data:

$$\frac{\Delta n(t)}{\Delta n_o} = C_1 e^{-k1t} + C_2 e^{-k2t}. \qquad (11)$$

Qualitative examination of Figure 4 reveals that the dual-rate kinetic model produces a fit of the data that accounts for both the total native birefringence and the changing decay rates.

Quantitative analysis of the dual-rate model has resulted in the working hypothesis that dynamic linear birefringence measurements provide feedback of the conformational state of collagen fibers during denaturation processes. Statistical analysis of the dual-rate versus the single-rate models results in the dual-rate model proving to be a significantly better model for the 50–56°C data of Figure 2. The 58°C and 60°C data sets, however, contain too few data points for any model-selection statistical test. Complete details of the model selection statistical tests are presented in Maitland [22]. A more physically relevant result than the statistics, however, is the correlation of the constants, C_1 and C_2, of equation 11 with the literature-cited values of native intrinsic and form birefringence. Recall that Stanworth and Naylor [13] reported that stromal lamellae have intrinsic and form birefringence contributions of 30% and 70%, respectively, of the total lamellar birefringence. Additionally, Bettlelhiem and Kaplan [23] reported 25% and 75% birefringence contributions for the intrinsic and form components of bovine stroma. The physical interpretation of these two birefringence constituents is that intrinsic birefringence is a molecular anisotropy property, whereas the form birefringence is a result of the anisotropy inherent to the ordered arrangement of collagen fibers. The weighted mean of the C_1 and C_2 coefficients of the dual-rate model fit of the 50–58°C data sets are 21 ± 2% and 79 ± 2%, respectively. Thus, we postulate that the dual-rate model is a mathematical description of the time-temperature dependence of the molecular and fibril structures of the RTT.

Acceptance of a dual-rate kinetic model implies that two sets of thermodynamic parameters are necessary to describe fully the birefringence-monitored denaturation of collagenous tissues. However, despite the improvements of the dual-rate fit over the single-rate fit, the single-rate results are still appropriate for discussion when the slower of the two reactions is under study. The quantitative thermodynamic results discussed below are for the single-rate fit.

Our results, in general, compare favorably with the results of other investigations. However, direct comparisons between our kinetic findings and the results of others show some discrepancies. The studies by Pearce et al. [3] and Jacques and Prahl [21] are representative of the application of kinetic analysis in the tissue-optics field and will serve as examples for our discussion of kinetic issues.

Pearce et al. [3] measured, from histologic sections, birefringence-induced intensity changes for rat skin exposed to various time-temperature histories. They found $A = e^{104}$ sec^{-1} and E_a = 73.2 kcal/mole, which are in general agreement with our values for RTT: $A = e^{129\pm1.2\ \text{sec}}$ sec^{-1} and $E_a = 88.5 \pm 0.8$ kcal/mole. Discrepancies between these values could be due to, e.g., differences in the cross-linking of the collagen fibers in RTT and rat skin that led to differences in the energy required to denature the collagen. Further, even though we have seen, in unpublished studies, that collagen linear birefringence dominates over the linear birefringence of other tissue constituents,

the elastin and similar components of skin also may effect intensity measurements dependent on linear birefringence. Thus we do not expect the kinetic parameters from 3-month-old RTT to match those found from rat skin (animal age not reported). In addition to the physical differences between the two tissues, our application of the Arrhenius integral deviates from the standard kinetic analysis used in the tissue-optics field and requires some discussion.

Using histologic sections of previously heated tissue, Pearce et al. [3,4] measured the intensity of broad-band light transmitted through a polarizer-tissue-analyzer set-up. The measured changes in intensity were due to phase shift changes that are coupled to changes in the tissue birefringence. One should note that in a nonscattering medium the measure intensity, I, is related to the phase shift, δ: $I = \sin^2(\delta/2)$ [8]. As indicated in equation 1, the phase shift is a function of both the linear birefringence, Δn, and the sample thickness, d. We have seen that collagen shrinkage, changes in the scattering losses, and Δn changes occur, for the same sample and same time-temperature history, at different kinetic rates [22]. That is, the kinetic sum-toll of birefringence-induced-interference intensity is a multiplicative combination of the kinetics attributed to birefringence and optical pathlength, where the latter is assumed equal to the thickness for optically thin samples. Pearce et al. [3,4] corrected for shrinkage by using sections of consistent thickness for their intensity measurements. Additionally, their application of the Arrhenius equation was blind to multiple kinetic reactions. However, we feel that multiple sequential or parallel reactions will be of significance only when birefringence-induced-interference intensity is measured dynamically, during the denaturation process.

Jacques and Prahl [21] used the rate constant formulation of the Arrhenius equation in the data reduction of the shrinkage of rat skin. At 62°C they reported $k = 0.036 \pm 0.026$ (s^{-1}). Using our E_a and A values presented above, equation 2 predicts $k = 0.033$ (s^{-1}) at 62°C. Our parameters do not fit their 64°C and 66°C data points as well as the 62°C k value, but, in general, Jacques and Prahl's data [21] follow a first-order reaction that is predicted by our parameters. However, conclusions drawn from this correlation are speculative given the small number of data points available. More importantly, neither investigation was designed to test the kinetic relationship between different conformational probes (i.e., test the differences between shrinkage and linear birefringence).

Finally, a note regarding the number of figures in our fitted kinetic parameters E_a and A is warranted. In order to accurately predict our experimental k values with equation 2, we determined that six figures must be maintained in reporting the E_a and A values. The need for such an extreme number of digits stems from the fact that equation 2 is, essentially, the subtraction of two nearly equal large exponents. Unfortunately, the inclusion of six significant figures has little physical relevance given that the standard error indicates an uncertainty in the estimate of E_a and A at the second or third decimal places. However, for the purpose of predicting rate constants or other similar applications of equation 2, we found $E_a = 88.5152$ kcal/mole and $A = e^{129.588}$ sec^{-1}.

In summary, we have shown that a real-time measure of changes in tissue linear birefringence can be used to monitor and quantify the tissue denaturation process. The application of the damage integral, which is given by equation 9, to denaturation processes assumes a first-order kinetic reaction [17]. The calculation of kinetic rate coefficients allows us to evaluate the reaction order and complexity (i.e., multiple reactions occurring simultaneously and/or sequentially). Thus we encourage other investigators to include the intermediate step of calculating the kinetic rate constants so that reaction order and complexity may be reported. Price and Dwek [17] concisely present the rate coefficient form of the Arrhenius equation. Further, the rate constant provides a means beyond the entropy and enthalpy, or the related activation energy and pre-exponential coefficient, by which various measures of kinetic changes can be compared (i.e., shrinkage, viscosity, optical measurements—polarized and unpolarized, scattering and absorption changes).

ACKNOWLEDGMENTS

This work was supported in part by a National Science Foundation Young Investigator Award BCS-9257492, National Science Foundation grant BCS-9222483, National Institutes of Health grant R01GM50534, and by the MRSEC Program of the National Science Foundation, at the Materials Research Center of Northwestern University, under Award No. DMR-9120521. All research for this report was performed at Northwestern University.

REFERENCES

1. Fawcett DW. "A Textbook of Histology," 11th ed. Philadelphia: Saunders, 1986.
2. Thompsen S, Pearce JA, Cheong WF. Changes in birefringence as markers of thermal damage in tissues. IEEE Trans on Biomed Eng 1989; BME-36(12):1174–1179.
3. Pearce J, Thomsen S, Vijverberg H, McMurray T. Kinetics for birefringence changes in thermally coagulated rat skin collagen. In: Bass LS, ed. "Lasers in Otolaryngology, Dermatology, and Tissue Welding." SPIE 1993, 1876: 180–186.
4. McMurray T, Han A, Pearce JA. Thermal damage quantification form tissue birefringence image analysis. In: Acharya RS, Goldgof DB, eds. "Biomedical Image Processing and Biomedical Visualization." SPIE 1993, 1905: 140–151.
5. Bloss FD. "An Introduction to the Methods of Optical Crystallography." Watson, NY: Holt, 1961.
6. McCrone WC, Delly JG. "The Particle Atlas: Volume, Principles and Techniques." Ann Arbor, MI: Ann Arbor Science, 1973.
7. Jerrard HG. Optical compensators for measurement of elliptical polarization. J Op Soc Am 1948; 38(1):35–59.
8. Patzelt WJ. "Polarized Light Microscopy, Principles, Instruments, Applications." Brochure published by Wetzlar, Germany: Ernst Leitz Wetzlar GmbH (Leica), 1985.
9. Cohen C. Optical rotation and helical polypeptide chain configuration in collagen and gelatin. J Biophys Biochem Cytol 1955; 1(3):203–214.
10. Yoshioka K, O'Konski CT. Electric properties of macromolecules. IX. Dipole moment, polarizability, and optical anisotropy factor of collagen in solution from electric birefringence. Biopolymers 1966; 4:499–507.
11. Naylor EJ. The structure of the cornea as revealed by polarised light. Quart J Micr Sci 1953; 94:83–88.
12. van Blokland GJ, Verhelst SC. Corneal polarization in the living human eye explained with a biaxial model. J Op Soc Am A 1987; 4:82–90.
13. Stanworth A, Naylor EJ. Polarised light studies in cornea. I. The isolated cornea. J Exp Biol 1953; 30:160–163.
14. Blout ER, Carver JP, Gross J. Intrinsic cotton effects in collagen and poly-L-proline. Biophys J 1963; 85:644–646.
15. Stryer L. Chapter 9: Connective-tissue proteins: Collagen, elastin, and proeoglycans. "Biochemistry." San Francisco: W.H. Freeman, 1975.
16. Hayashi T, Curran-Patel S, Prockop DJ. Thermal stability of the triple helix of type I procollagen and collagen. Precautions for minimizing ultraviolet damage to proteins during circular dichroism studies. J Am Chem Soc 1979; 18:4182–4187.
17. Price NC, Dwek RA. "Principles and Problems in Physical Chemistry for Biochemists." Oxford: Clarendon Press, 1974.
18. Birngruber R. Thermal modeling in biological tissues. In Hillenkamp F, Pratesi R, Sacchi CA, eds, "Lasers in Biology and Medicine." New York: Plenum Press, 1979, pp 77–97.
19. Welch AJ. The thermal response of laser irradiated tissue. IEEE J of QE 1984; QE-20:1471–1481.
20. Draper NR and Smith H. "Applied Regression Analysis." New York, J Wiley & Sons, 1966.
21. Jacques SL, Prahl SA., "Modeling optical and thermal distributions in tissues during laser irradiation." Lasers Surg Med 1987, 6:494–503.
22. Maitland DJ, Ph.D. thesis, Dynamic Measurements of Tissue Birefringence: Theory and Experiments, Northwestern University, 1995.
23. Bettelheim FA, Kaplan D. Small angle light scattering of bovine cornea as affected by birefringence. Biochim Biophys Acta 1973, 313:268–276.